

# Structural investigation of the effect of annealing temperature on the Fe:WO<sub>3</sub> structure on a silicon substrate

Sevda SARITAŞ<sup>1</sup>

<sup>1</sup> Department of Electric and Energy, İspir Hamza Polat Vocational School, Atatürk University, Erzurum, Türkiye

## ABSTRACT

In this study, iron-doped tungsten oxide (Fe: WO<sub>3</sub>) thin films were synthesized on p-type silicon (Si (111)) and glass substrates using a DC/RF co-magnetron sputtering technique under controlled deposition conditions. The effect of post-deposition annealing on the structural and crystallographic evolution of the films was systematically examined at temperatures of 550°C, 650°C, and 750°C in air. X-ray diffraction (XRD) analysis revealed that the as-deposited films were poorly crystalline. In contrast, progressive annealing resulted in a significant enhancement in crystallinity, accompanied by the formation of a well-defined monoclinic WO<sub>3</sub> phase. Increasing the annealing temperature led to sharper diffraction peaks and larger grain sizes, confirming thermally induced grain growth and improved structural ordering. A noticeable shift of diffraction peaks toward higher 2θ values was observed with Fe incorporation, indicating lattice contraction due to the substitution of W<sup>6+</sup> ions by smaller Fe<sup>3+</sup> ions, as well as the generation of oxygen vacancies for charge compensation. The average crystallite size increased from 21.6 nm at 550°C to 62.4 nm at 750°C, demonstrating that Fe doping promotes thermally assisted grain coalescence. These results suggest that Fe incorporation effectively alters the lattice parameters and structural stability of WO<sub>3</sub> without creating any secondary Fe-based oxide phases. Overall, these findings provide valuable insights into the relationship between microstructural evolution and dopant-induced modifications in Fe: WO<sub>3</sub> systems, paving the way for optimizing their performance in photocatalytic and gas-sensing applications.

**Keywords:** WO<sub>3</sub>, X-ray diffraction (XRD), DC/RF co-magnetron sputtering

## INTRODUCTION

Tungsten oxide (WO<sub>3</sub>) is a multifunctional transition metal oxide that has gained significant attention due to its outstanding electrical, optical, and chemical characteristics. As an n-type semiconductor, WO<sub>3</sub> possesses a moderate bandgap typically between 2.6 and 3.2 eV, which enables efficient absorption of visible light and supports various photoactive processes. Its relatively high electron mobility and moderate hole diffusion length facilitate effective charge separation, making the material suitable for optoelectronic and energy-related devices. In addition to these intrinsic advantages, WO<sub>3</sub> is chemically robust, resistant to corrosion, non-toxic, and widely available—features that collectively promote its use in sustainable technologies such as electrochromic coatings, smart windows, photocatalysts, and gas-sensing systems. The physical and functional behavior of WO<sub>3</sub> can be tuned through several engineering approaches, including modification of the crystal structure, surface morphology, and electronic configuration. Among these, elemental doping has emerged as one of the most effective strategies to adjust its electronic and optical properties. Through doping, parameters such as carrier concentration, conductivity, defect density, and bandgap width can be tailored to meet specific application requirements. Iron (Fe) is considered an efficient dopant for WO<sub>3</sub> because of the close ionic radius match between Fe<sup>3+</sup> (0.64 Å) and W<sup>6+</sup> (0.62 Å). This similarity allows Fe ions to substitute tungsten sites with minimal lattice distortion. The incorporation of Fe atoms tends to generate oxygen vacancies, which act as shallow donor states, enhancing electrical conductivity and facilitating light absorption by narrowing the bandgap. These alterations improve the functional efficiency of WO<sub>3</sub> in photocatalytic and gas-sensing applications.<sup>1–3</sup>

Despite numerous studies exploring Fe: WO<sub>3</sub>, the literature still presents inconsistent findings regarding its structural response and crystallinity. Some researchers report enhanced structural order following Fe substitution, while others observe partial amorphization or lattice disorder. These discrepancies suggest that the effects of Fe incorporation depend strongly on synthesis parameters and dopant concentration. Consequently, a systematic investigation of the structural evolution and phase behavior of Fe-doped WO<sub>3</sub> thin films remains crucial for clarifying these effects and optimizing the material for advanced functional use. The deposition method plays a decisive role in determining the physical and electronic features of WO<sub>3</sub> films. Techniques such as sol–gel processing, chemical vapor deposition (CVD), atomic layer deposition (ALD), and various physical vapor deposition (PVD)



Received 14.10.2025  
Revision Requested 07.12.2025  
Last Revision 08.12.2025  
Accepted 11.12.2025  
Publication Date 31.12.2025

## Corresponding author:

Sevda SARITAŞ

## E-mail:

sevda.saritas@atauni.edu.tr

Cite this article: Saritas S. Structural investigation of the effect of annealing temperature on the Fe:WO<sub>3</sub> structure on a silicon substrate. *NanoEra*. 2025;5(2):50-54



Content of this journal is licensed under a Creative Commons Attribution-NonCommercial-NoDerivatives 4.0 International License.

methods have been employed to obtain high-quality  $\text{WO}_3$  coatings. Among them, direct current (DC) magnetron sputtering offers significant advantages, including precise control of film composition and thickness, strong adhesion to the substrate, high deposition rates, and excellent film uniformity. Furthermore, this approach enables the fabrication of nanostructured films possessing a large surface-to-volume ratio, which is beneficial for enhancing gas adsorption, catalytic activity, and charge transfer processes.<sup>4–7</sup>

The co-sputtering configuration provides an additional advantage by allowing simultaneous control of the base material and dopant content. Incorporating metallic elements such as Pd, Pt, Au, Cu, Ag, or Fe during sputtering has been demonstrated to modify the concentration of oxygen vacancies and to fine-tune the electronic structure of  $\text{WO}_3$ , thereby improving its gas selectivity and photoactivity. Among these, Fe doping has been reported to significantly enhance the response of  $\text{WO}_3$ -based films toward gases such as ozone ( $\text{O}_3$ ), carbon monoxide (CO), and ethanol ( $\text{C}_2\text{H}_5\text{OH}$ ).<sup>8–10</sup>

In the present work, Fe-doped  $\text{WO}_3$  thin films were deposited by a DC-RF co-magnetron sputtering technique under controlled experimental conditions. The structural and microstructural evolution of the films was systematically characterized to elucidate the influence of Fe incorporation on the crystallinity and phase composition of  $\text{WO}_3$ . The outcomes of this study aim to deepen the understanding of structure–property relationships in Fe-modified  $\text{WO}_3$  systems and to establish a foundation for optimizing their performance in photocatalytic and gas-sensing applications.

The novelty of this study lies in the systematic investigation of Fe:  $\text{WO}_3$  thin films. These films were deposited by a DC/RF co-magnetron sputtering technique. The focus is on post-deposition annealing effects on structural evolution on both silicon and glass substrates. Unlike previous works that often used sol-gel or chemical deposition methods, this study emphasizes precise physical vapor deposition parameters. It correlates these with temperature-induced crystallographic transformations, providing new insights into dopant-driven grain growth mechanisms and phase stability under controlled thermal conditions.

## MATERIALS and METHOD

Fe-doped tungsten oxide (Fe:  $\text{WO}_3$ ) thin films were deposited onto polished p-type silicon (Si) (111) and glass substrates using a DC/RF co-magnetron sputtering system. High-purity tungsten (99.99%) and iron (99.99%) metallic targets served as the sputtering sources. Prior to deposition, the Si and glass substrates were cleaned ultrasonically in acetone, ethanol, and deionized water for 10 minutes each, followed by drying with nitrogen gas.

Figure 1 provides a detailed overview of a reactive RF/DC magnetron co-sputtering system, expertly configured for the deposition of a Fe:  $\text{WO}_3$  thin film.<sup>11</sup> This advanced system features two carefully selected sputtering targets: a two-inch tungsten (W) target and an iron (Fe) target, both exhibiting an exceptional purity level of 99.99%. These high-purity targets are

securely mounted on dedicated RF and DC sputtering guns, which are designed to optimize the deposition process and ensure consistent film quality.

The target-substrate holder, with a precise diameter of approximately 57 mm, is designed for stability and accuracy. The deposition angle is meticulously fixed at 45 degrees, allowing for optimal deposition geometry, which helps in achieving uniform thin film coverage across the substrate.

To create the ideal vacuum environment necessary for high-quality film deposition, the chamber is first evacuated using a highly efficient molecular turbo pump, which successfully establishes an ultra-low base pressure of  $5 \times 10^{-6}$  Torr. Once this vacuum level is achieved, an argon flow rate of 50 standard cubic centimeters per minute (sccm) is introduced into the chamber. This process raises the working pressure to the target level of  $8.3 \times 10^{-3}$  Torr, facilitated by a precisely controlled mixture of argon and oxygen gases ( $\text{Ar}/\text{O}_2$ ), which is crucial for the subsequent formation of the desired oxide film.

Prior to the actual deposition phase, a critical pre-sputtering process is conducted to ensure the purity and cleanliness of the target surfaces. This process lasts for 15 minutes and is conducted at RF and DC power levels of 100 watts. The pre-sputtering serves not only to remove any contaminants but also to condition the target surfaces, ensuring optimal sputtering performance. During this vital stage, the substrates are meticulously shielded by an electronic shutter, preventing any undesired exposure to sputtering particles.

In addition, the substrate holder is equipped with a sophisticated rotation system, which is set to a consistent speed of 2 revolutions per minute (rpm) throughout the entire deposition process. This rotation enhances the uniformity of the coating by ensuring that all areas of the substrate are evenly exposed to the sputtered material. To maintain stability in the sputtering process, the DC voltage is set firmly at 75 watts, while the RF voltage is kept constant at 100 watts. These carefully controlled parameters are essential for achieving high-quality Fe:  $\text{WO}_3$  thin films with the desired properties.

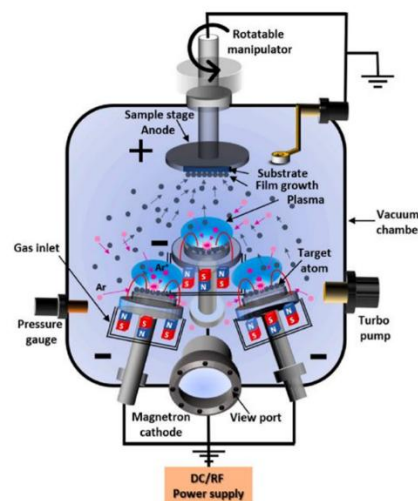


**Figure 1.** Experimental setup for Fe:  $\text{WO}_3$  deposition using RF/DC magnetron sputtering system.<sup>11</sup>

The total deposition time lasted 60 minutes, resulting in films with an average thickness of the thin films was measured to be 480-500 nm with the utmost precision using the "Kla Tencor Stylus Profiler P7" device. All films were grown at room temperature without intentional substrate heating to minimize unwanted interdiffusion effects.

After deposition, the as-deposited Fe: WO<sub>3</sub> thin films were annealed in ambient air at three different temperatures: 550°C, 650°C, and 750°C, for 1 hour using a programmable muffle furnace. Additionally, some of the as-deposited Fe: WO<sub>3</sub> thin films on glass substrates were also annealed in ambient air at 550°C for 1 hour. The heating rate was set to 5°C per minute, and the samples were allowed to cool naturally to room temperature inside the furnace. This post-annealing process was conducted to promote crystallization, relieve internal stresses, and investigate the temperature-dependent structural evolution of the Fe-doped WO<sub>3</sub> films.

The crystal structure and phase composition of the films were examined using X-ray diffraction (XRD) analysis, employing a Cu K $\alpha$  radiation source ( $\lambda = 1.5406 \text{ \AA}$ ) operated at 30 kV and 10 mA. Measurements were conducted over a  $2\theta$  range of 15° to 75°, using a step size of 0.02° and a scan rate of 1° per minute. The resulting diffraction patterns were analyzed to identify the crystalline phases, evaluate preferred orientations, and estimate the average crystallite size using the Scherrer equation. Furthermore, the impact of annealing temperature on the structural evolution and phase stability of the Fe: WO<sub>3</sub> films was systematically investigated. The parameters characterizing the structural properties of the Fe: WO<sub>3</sub> structure are given in detail in Table 1.

**Table 1.** Parameters characterizing the structural properties of the Fe: WO<sub>3</sub> structure on glass at 550°C

Pos. [°2Th.]	hkl	d-spacing [Å]	Rel. Int. [%]	FWHM [°2Th.]
23,6941	110	3,75518	100,00	0,3633
29,1820	012	3,06027	18,15	1,2931
33,8820	-112	2,64575	33,52	0,3824
47,8820	004	1,89981	9,41	0,4635
50,8366	014	1,79612	12,21	0,4981
54,0187	213	1,69759	9,43	0,4277

## RESULTS

X-ray diffraction (XRD) was utilized to examine the crystalline structure and phase evolution of Fe: WO<sub>3</sub> thin films that were annealed at various temperatures. Figure 2 illustrates the XRD patterns of the as-deposited films as well as those annealed at temperatures of 550°C, 650°C, and 750°C in air. The as-deposited films exhibited a broad and low-intensity diffraction peak centered around  $2\theta \approx 23^\circ$ , indicating their crystalline nature.

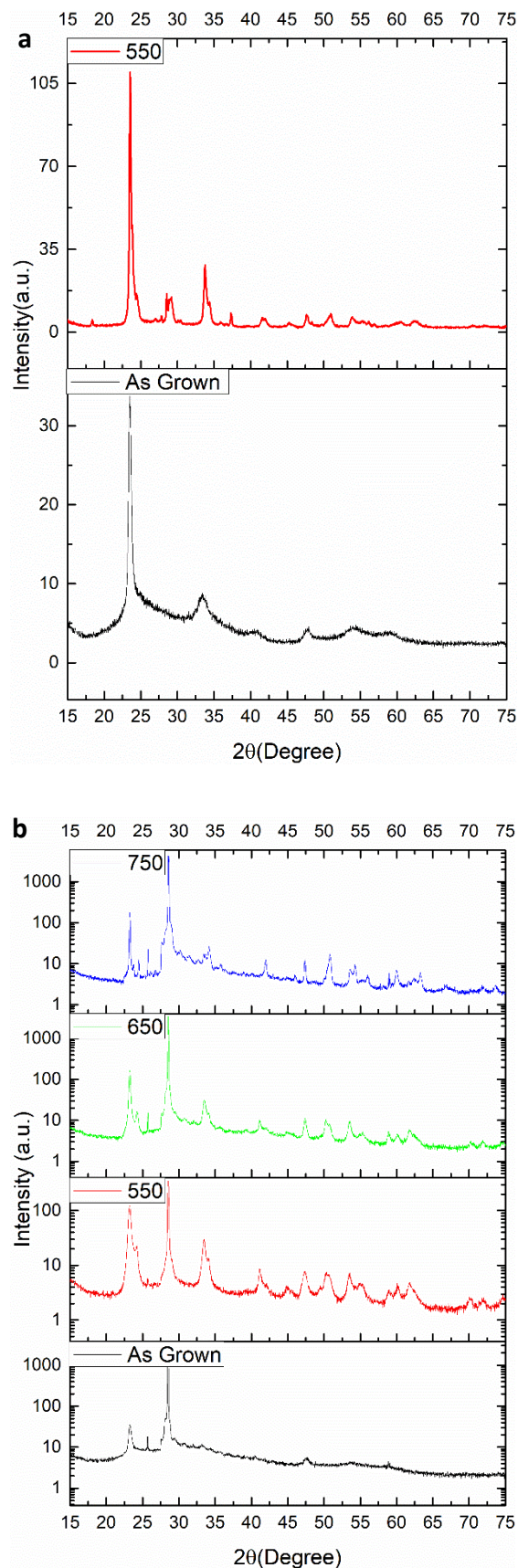


**Figure 2.** XRD patterns of films of Fe: WO<sub>3</sub> structure grown on glass substrate (a) and silicon substrate (b).

Upon annealing, the diffraction peaks became sharper and more intense, demonstrating a progressive improvement in crystallinity with increasing temperature. At 550°C, diffraction peaks corresponding to the (110), (012), and (004) (Figure 2, Figure 3) planes emerged, confirming the formation of monoclinic WO<sub>3</sub> (Reference Code. 01-0880-550) and Si (Reference Code. 01-0810-068). As the annealing temperature increased to 650°C, these peaks became more pronounced, and additional reflections, such as (014) (Figure 4) appeared, indicating enhanced crystallization and grain growth.

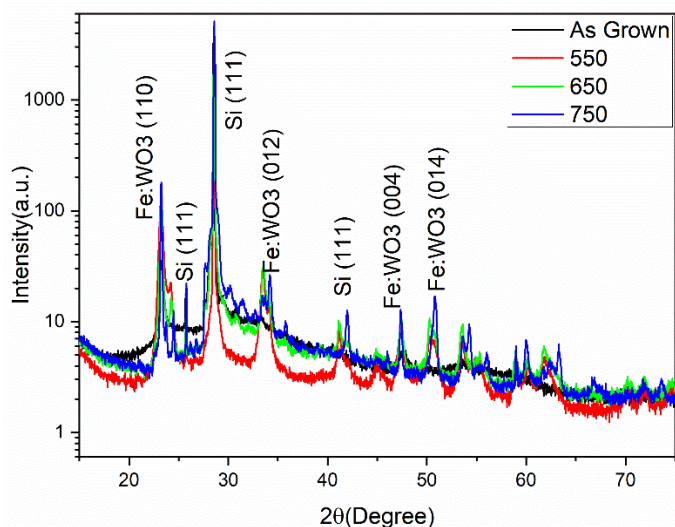


**Figure 3.** XRD patterns and Miller index values of films grown on silicon substrate of Fe: WO<sub>3</sub> structure at different annealing temperatures.

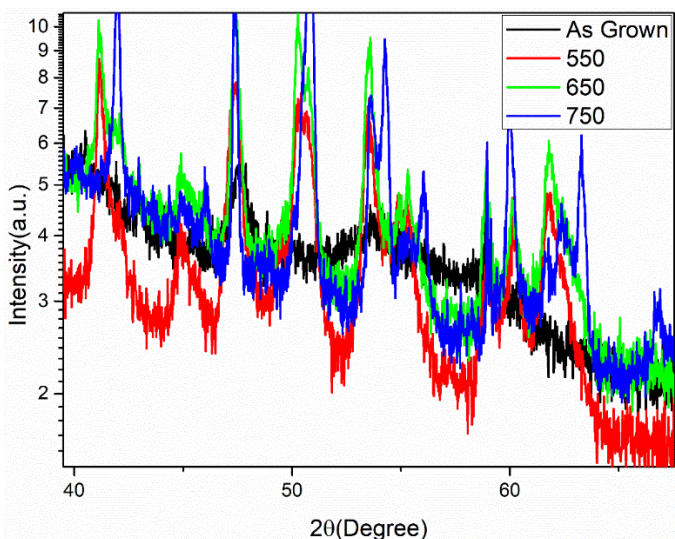


**Figure 4.** Detailed representation of XRD patterns and peak shifts of films grown on silicon substrate of Fe: WO<sub>3</sub> structure at different annealing temperatures.

The increase to 750°C resulted in the sharpest and most well-defined diffraction peaks, suggesting the development of highly crystalline monoclinic WO<sub>3</sub>. Importantly, no secondary phases such as Fe: WO<sub>3</sub> were detected within the limits of the XRD system. This finding suggests that Fe atoms were successfully incorporated into the WO<sub>3</sub> lattice without forming separate oxide phases.

A slight shift of the diffraction peaks toward higher 2θ angles was observed in the Fe-doped samples compared to undoped WO<sub>3</sub> (reference data). This shift can be attributed to lattice contraction resulting from the substitution of W<sup>6+</sup> ions (0.62 Å) by smaller Fe<sup>3+</sup> ions (0.64 Å), as well as the possible generation of oxygen vacancies to maintain charge neutrality. This observation is consistent with previous reports on Fe: WO<sub>3</sub> systems.

The average crystallite size (D) of the annealed films was estimated from the full width at half maximum (FWHM) of the (110) diffraction peak using the Scherrer equation:

$$D = K\lambda / \beta \cos\theta \quad (1)$$

where  $K = 0.9$ ,  $\lambda = 1.5406 \text{ \AA}$ ,  $\beta$  is the FWHM in radians, and  $\theta$  is the Bragg angle. The calculated crystallite size increased from approximately 21.6 nm at 550°C to 36.9 nm at 650°C, reaching ~62.4 nm at 750°C, confirming that higher annealing temperatures facilitate grain growth and densification.

Although the ionic radius of Fe<sup>3+</sup> (0.64 Å) is slightly larger than that of W<sup>6+</sup> (0.62 Å), a shift in the XRD peaks toward higher 2θ values was observed in the Fe-doped WO<sub>3</sub> films. This apparent lattice contraction cannot be explained solely by ionic substitution. Several studies have suggested that such peak shifts can also result from the creation of oxygen vacancies and local lattice distortions during doping and annealing. These factors may collectively lead to net lattice shrinkage, despite the presence of slightly larger dopant ions.<sup>1,7</sup> Moreover, the non-equilibrium conditions of magnetron sputtering—especially under reactive atmospheres—can promote the formation of structural defects that influence the lattice parameter.<sup>8</sup> These effects have been previously reported in Fe-doped and other metal-doped WO<sub>3</sub> systems. Dopant-induced lattice strain and oxygen-deficiency environments can modify the crystalline structure.<sup>4,5</sup> Therefore, the observed contraction is more likely a complex consequence of defect chemistry, rather than ionic radius mismatch alone.

## CONCLUSION

The observed structural improvements—such as increased crystallite size, enhanced crystallinity, and the formation of oxygen vacancies—are expected to significantly influence the functional performance of Fe-doped WO<sub>3</sub> films in gas sensing and photocatalysis. Larger crystallite sizes and improved structural ordering enhance electron transport by reducing grain boundary scattering, which is beneficial for charge separation in photocatalytic reactions. Simultaneously, oxygen vacancies created through Fe<sup>3+</sup> substitution play a dual role: they act as

shallow donor states to enhance electrical conductivity and serve as active adsorption sites for gas molecules, thereby improving gas-sensing response. These combined effects underscore the critical importance of optimizing annealing temperature and dopant incorporation for tailoring the material's application-specific performance.

These findings highlight the crucial role of thermal annealing in enhancing the crystallization of Fe: WO<sub>3</sub> films and improving their structural ordering. The incorporation of Fe ions not only modifies the lattice parameters but also influences the nucleation process during grain growth, which may subsequently affect the optical and electrical properties of the films. Thus, the observed temperature-dependent structural evolution offers valuable insights for optimizing processing conditions for Fe: WO<sub>3</sub> films, particularly for applications in gas sensing and photocatalysis.

**Peer-review:** Externally peer-reviewed.

**Conflict of Interest:** The author have no conflicts of interest to declare.

**Financial Disclosure:** The author declared that this study has received no financial support.

**Use of Artificial Intelligence:** The author declare that Artificial Intelligence is (not) Used except for grammar check.

## REFERENCES

- Al-Kuhaili MF, Drmosh QA. Investigating the structural and optoelectronic properties of co-sputtered Fe-doped WO<sub>3</sub> thin films and their suitability for photocatalytic applications. *Mater Chem Phys*. 2022;281:125897. doi:10.1016/j.matchemphys.2022.125897
- Tesfamichael T, Piloto C, Arita M, Bell J. Fabrication of Fe-doped WO<sub>3</sub> films for NO<sub>2</sub> sensing at lower operating temperature. *Sensors Actuators B Chem*. 2015;221:393-400. doi:10.1016/j.snb.2015.06.090
- Ramkumar S, Rajarajan G. Effect of Fe doping on structural, optical and photocatalytic activity of WO<sub>3</sub> nanostructured thin films. *J Mater Sci Mater Electron*. 2016;27(2):1847-1853. doi:10.1007/s10854-015-3963-6
- Osiac M, Cioatera N, Jigau M. Structural, Morphological, and Optical Properties of Iron Doped WO<sub>3</sub> Thin Film Prepared by Pulsed Laser Deposition. *Coatings*. 2020;10(4):412. doi:10.3390/coatings10040412
- Tesfamichael T, Ponzoni A, Ahsan M, Faglia G. Gas sensing characteristics of Fe-doped tungsten oxide thin films. *Sensors Actuators B Chem*. 2012;168:345-353. doi:10.1016/j.snb.2012.04.032
- Chaudhari AK, Singh VB. Mechanical and physical properties of electrodeposited Ni-Fe, WO<sub>3</sub> doped nanocomposite. *Surf Coatings Technol*. 2016;307:683-692. doi:10.1016/j.surfcoat.2016.09.072
- Ouadah E, Hamdadou NE, Ammari A. Morphological, Structural and Optical Properties of Fe-Doped WO<sub>3</sub> Films Deposited by Spray-Pyrolysis. *J Electron Mater*. 2022;51(1):356-369. doi:10.1007/s11664-021-09300-0
- Dhunna R, Koshy P, Sorrell CC. Effect of Iron Doping on the Mineralogical, microstructural, Optical, and Chemical Properties of WO<sub>3</sub> Thin Films. *J Aust Ceram Soc Vol*. 2015;51(2):18-22.
- Yin Y, Lan C, Hu S, Li C. Effect of Gd-doping on electrochromic properties of sputter deposited WO<sub>3</sub> films. *J Alloys Compd*. 2018;739:623-631. doi:10.1016/j.jallcom.2017.12.290
- Piloto C, Shafiei M, Khan H, Gupta B, Tesfamichael T, Motta N. Sensing performance of reduced graphene oxide-Fe doped WO<sub>3</sub> hybrids to NO<sub>2</sub> and humidity at room temperature. *Appl Surf Sci*. 2018;434:126-133. doi:10.1016/j.apsusc.2017.10.152
- Salari MA, Şenay V, Muğlu GM, Sarıtaş S, Kundakçı M. Evaluation of the optical, structural, and morphological characteristics of a Sn-doped α-Fe<sub>2</sub>O<sub>3</sub> thin film fabricated using RF and DC magnetron Co-sputtering technique. *Ceram Int*. 2025;51(17):23068-23076. doi:10.1016/j.ceramint.2025.02.410